

## New metal connectors developed to improve the shear strength of stone masonry walls

Turan Karabork<sup>\*1</sup> and Yilmaz Kocak<sup>2a</sup>

<sup>1</sup>*Division of Structures, Department of Civil Engineering, Aksaray University, 68100, Aksaray, Turkey*

<sup>2</sup>*Inspection and Control Expert, Ministry of Defense, 06000, Ankara, Turkey*

*(Received October 10, 2013, Revised February 11, 2014, Accepted February 15, 2014)*

**Abstract.** Stone masonry structures are widely used around the world, but they deteriorate easily, due to low shear strength capacity. Many techniques have been developed to increase the shear strength of stone masonry constructions. The aim of this experimental study was to investigate the performance of stone masonry walls strengthened by metal connectors as an alternative shear reinforcement technique. For this purpose, three new metal connector (clamp) types were developed. The shear strength of the walls was improved by applying these clamps to stone masonry walls. Ten stone masonry walls were structurally tested in diagonal compression. Various parameters regarding the in-plane behavior of strengthening stone masonry walls, including shear strength, failure modes, maximum drift, ductility, and shear modulus, were investigated. Experimentally obtained shear strengths were confirmed by empirical equations. The results of the study suggest that the new clamps developed for the study effectively increased the levels of shear strength and ductility of masonry constructions.

**Keywords:** stone masonry wall; clamp; diagonal testing; strengthening; shear strength; failure

### 1. Introduction

Even though stone masonry buildings represent a significant portion of the building stock worldwide, most of the existing stone masonry buildings are seismically vulnerable and should be reinforced. The basic structural elements that resist earthquakes in such buildings are the older stone masonry walls, which were intended to resist mainly lateral loads. Stone masonry structures are remarkably durable and they can resist fire, water, and insect damage. Masonry structures require few materials to build, the buildings can be easily repaired, and the material used is readily available and recyclable.

The seismic vulnerability of stone masonry buildings strongly depends on their ability to resist shear forces. The structural reliability of buildings can be estimated, and convenient strengthening techniques can be appropriately based upon the known in-plane shear behavior. Numerous techniques and materials have been developed to increase the shear capacity of stone masonry structures. In recent decades, the use of fiber reinforced polymers (FRP) became a valid method

---

<sup>\*</sup>Corresponding author, Ph.D., E-mail: [turankarabork@gmail.com](mailto:turankarabork@gmail.com)

<sup>a</sup>Civil Engineer

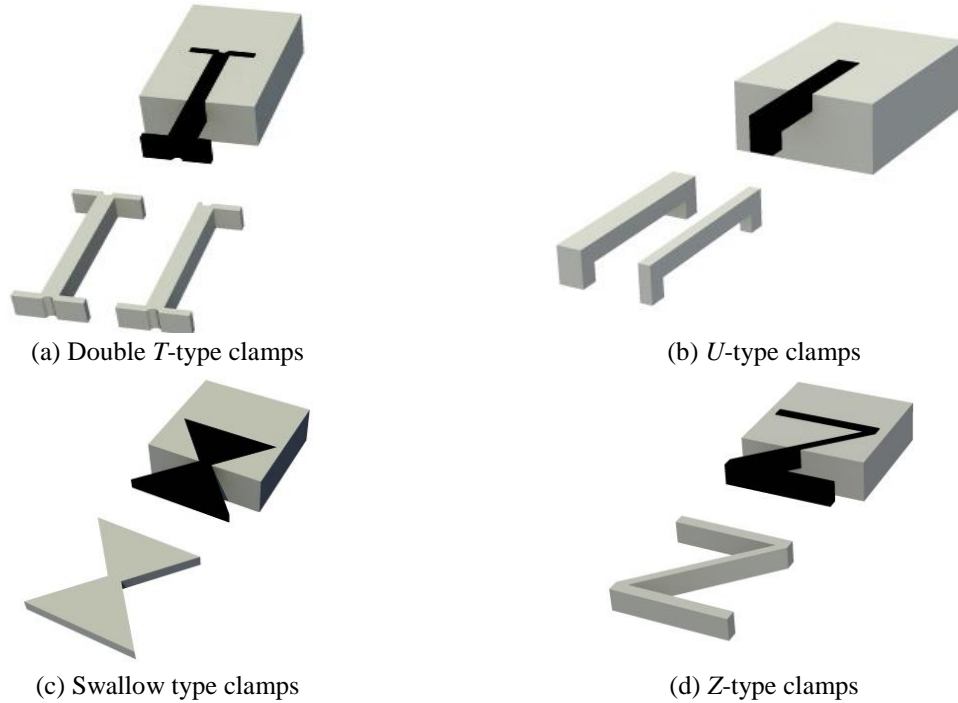


Fig.1 Different type of clamps

for retrofitting and strengthening structures (Altin *et al.* 2006, El Gawady *et al.* 2006). A large number of FRP masonry strengthening applications have been performed using either FRP bars or laminates. However, little analytical or experimental research has been conducted to investigate the strength of FRP strengthened masonry under shear forces (Gabor *et al.* 2006, Kalali and Kabir 2012). Several numerical studies have investigated the use of high strength twisted stainless steel reinforcement to increase the strength of masonry brick walls under shear force (Ismail *et al.* 2011, Ismail *et al.* 2012). There are only a few experimental results on the behavior of stone masonry walls. For instance, Chiostrini and Vignoli (1992) addressed strength properties and Tomazevic (1999) reported tests on strengthening and improvement of seismic performance of stone masonry walls. Corradi *et al.* (2003) performed an experimental study of the strength properties of double-leaf roughly cut stone walls by means of in-situ diagonal compression and shear-compression tests. Shariati *et al.* (2012) present an evaluation of the structural behavior of C-shaped angle shear connectors, which are suitable for transferring shear forces in composite structures in composite beams.

Stone masonry walls are made of a material that performs well in compression but has less shear and tensile strength. Therefore, various clamps are used in masonry walls to increase strength against shear forces (Fig. 1). The stone blocks are horizontally connected with clamps and are vertically connected with dowels (Fig. 2). Ancient builders placed metal connectors in most of the stone members between the columns' drums. These connectors were made of iron and were placed into mortises that were cut in the stone at unseen positions. The iron connectors were coated in lead to protect them from corrosion. At first, double-T clamps were used to connect all of the stone blocks in the horizontal direction. The objective of the connectors was to enable the

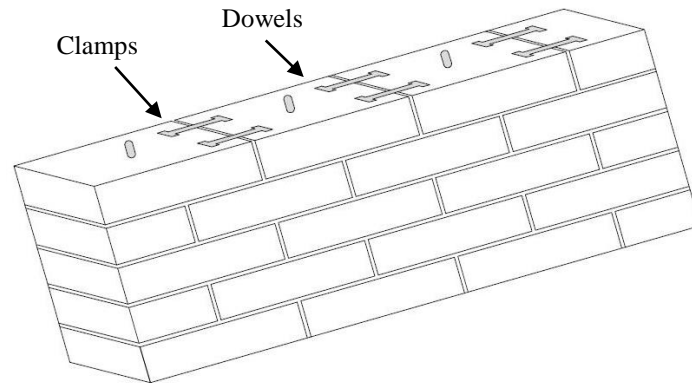


Fig. 2 Placement of metal connectors (clamps and dowels) into stones



(a) from the minaret of Murat Pasa Mosque in Skopje-Macedonia



(b) from the a stone arch bridge in Venetian-Italy



(c) from the church of Canli (Bell Church) in Aksaray-Turkey

Fig. 3 The samples of using clamps for various historical buildings

building to maintain its structure and stability in situations in which significant earthquake loads caused the friction ties and interlocking between the stone blocks to break. Metal connectors start helping with friction forces as soon as the first relative displacements of the blocks occur by providing plasticity to the building because the connectors allow the building to dissipate energy by deforming plastically (Papadopoulos 2006).

Metal clamps have been used since the early ages (Fig. 3). Currently, Toumbakari (2008) carried out a numerical study that concluded that the mechanical action of the connectors could explain the observed structural pathology, meaning rust might not be a necessary condition for structural failures to occur. Several studies have been carried out investigating new clamp types. Papadopoulos (2006) developed double-T clamps made of titanium with the goal that they be as ductile as possible in case the connection fails. Kourkoulis and Pasiou (2009) investigated the mechanical behavior of “I-shaped” clamps and their marble body surroundings when the epistyles are subjected to shear.

In this study, the behavior of various new types of clamps under shear was investigated. Three new clamp types were developed and tested. Experimental tests were performed to investigate the shear behavior in the application of one and two clamps. The clamp width was first used as a

variable parameter, but it was found to have no effect on the results. Therefore, a constant width is chosen. The results were compared to the test case in which no connectors were used, and the effectiveness of the clamps was obtained. The experimental results were compared with results obtained using empirical equations.

## 2. Experimental study

Testing was undertaken to investigate the in-plane performance of stone masonry walls strengthened using different types of clamps. Ten different masonry wall models were tested in induced diagonal compression. For each test, a different reinforcement connector was used to strengthen the stone masonry walls.

### 2.1 Material properties

Mechanical properties of stone masonry walls depend on the characteristics of the constituent elements, such as the stone and mortar, and on the interfacial interaction within the assemblage. The main mechanical properties of stone were determined by compressive and shear tests. Tuff stones taken from Hasan Mountain, a volcanic mountain in Aksaray, Turkey were used as a stone masonry wall component. Tuff stones are largely used in seismic regions, such as Italy, Turkey, and Japan (Augenti and Parisi 2011). The mechanical properties of six tuff stone specimens with 50×50×50 mm dimensions are determined according to TSE 699 standard. The mechanical properties of tuff stones are given comparatively on Table 1.

Table 1 Mechanical property of tuff stone

Test Type	This study	Augenti and Parisi 2010
Hardness (Mohs)	3	-
Hardness (Digital Schmidt)	35	-
Unit Volume Weight - Dry (kN/m <sup>3</sup> )	19.70	12.5
Unit Volume Weight - Saturated (kN/m <sup>3</sup> )	15.20	-
Porosity (%)	22.78	-
Water Absorption by Weight (%)	15	-
Humidity (%)	1.15	-
Color	Gray	Yellow
Ratio of Fullness (%)	76	-
Ultrasonic Velocity ( $\mu$ s)	60	-
Ultrasonic Velocity (km/s)	5.40	-
pH (in 100 mL water)	8.87	-
Water Soluble Salt Content (in 25 mL water) ( $\mu$ S)	590	-
Water Soluble Salt Content (in 25 mL water) (%)	0.58	-
Strength to Blow (MPa)	2.30	-
Uniaxial Compressive Strength (MPa)	12.70	4.13
Young modulus (MPa)	1600	1540
Shear modulus (MPa)	650	444

Table 2 Mechanical properties of Khorassan mortar

	Khorassan mortar
Compressive strength (MPa)	2.39
Young modulus (MPa)	1420
Shear modulus (MPa)	584

Khorassan, a traditional mortar that does not contain cement, was used as a mortar. Khorassan mortar is usually produced by using slaked lime as a binder, and various proportions of sand and stone powder as aggregates. Optionally, other organic and inorganic materials are mixed into the mortar to improve the quality of the mixture (Arioglu and Acun 2006). Mortars containing lime were used widely from the times of the ancient Greeks, Romans and Ottomans until the invention of hydraulic cement. During the age of the Ottoman Empire, the lime was mixed with water to form slaked lime and was heated and sifted for use in mortars. In addition, egg whites, hydraulic brick pieces or powder, and straw particles were added to the mixture (Isikdag and Topcu 2013). To simulate the stone masonry of ancient buildings, the mortar needed to have low-to-medium mechanical characteristics and consistency. The Khorassan mortar used for this study had a mix proportion of 1/2/1/1 by volume for sand/hydraulic lime/tuff stone powder/4 mm crushed tuff stone. To determine the compressive strength of the mortar, a 70×70×70 mm specimen was used with respect to TS EN 196-1. Additionally, the shear modulus of the mortar was obtained by applying a one-point loading flexure test to a 70×70×280 mm size specimen (TS EN 196-1). The experimentally obtained mechanical properties of Khorassan mortars are given of Table 2.

## 2.2 Test set-up and loading protocol

To investigate the in-plane diagonal shear strength, ASTM E-519-02 (2002) standard guidelines were used. The diagonal compression load was applied to the corners of the stone walls using double-effect hydraulic jack. The experimental setup for the diagonal compression load is shown in Fig. 4. The load is gradually applied using a hydraulic jack with a 500-kN load capacity. Testing machine is capable of displacement and force controlled loading. In this study, the tests were executed through force control mode with an average loading rate of 0.3 kN/sec until ultimate load. After ultimate load, displacement control mode with an average displacement was executed with rate of 5 mm/sec. Lateral and horizontal displacements of the compressed and stretched diagonals of the masonry walls were measured by LVDT transducers. The experimental results in the following sections were compared to the shear stress-drift curves of the compressed diagonals and to the damage distribution on the walls.

## 2.3 Masonry stone walls description

The masonry stone walls used for the diagonal compression tests were constructed pursuant to the RILEM (1994) recommendations. A series of ten stone masonry walls with dimensions of 650×730×150 mm were built for the tests. The walls were made of natural yellow stones with dimensions of 100×150×200 mm and had 10 mm of mortar between the stones. One of the walls did not have reinforcement (W00), and the two stone walls (W01 and W02) were strengthened only with dowels. One of the models (W41) used 30 mm wide clamps, while the other six models

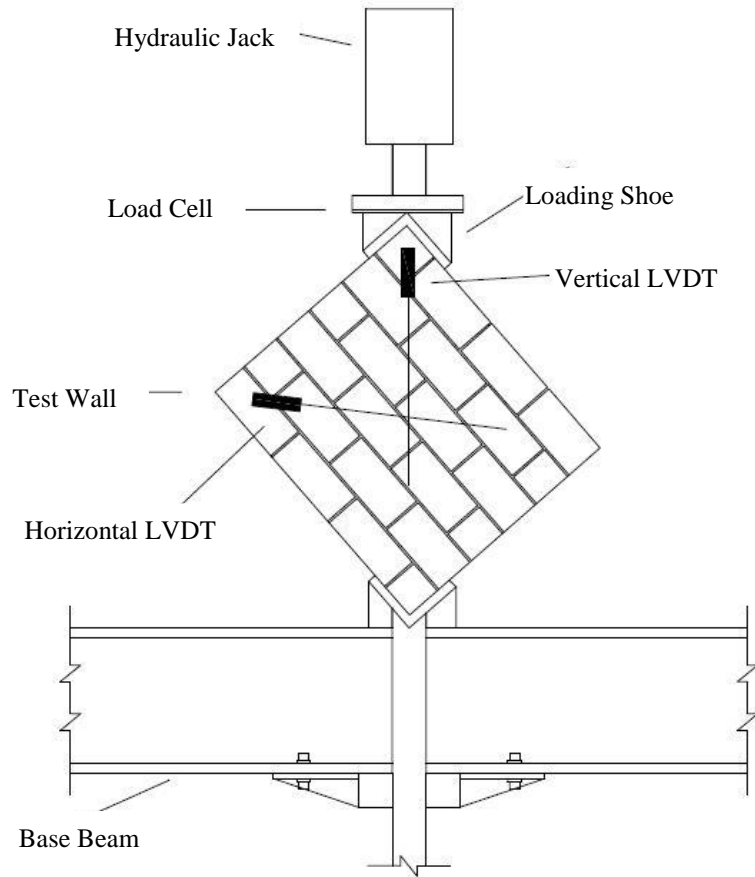
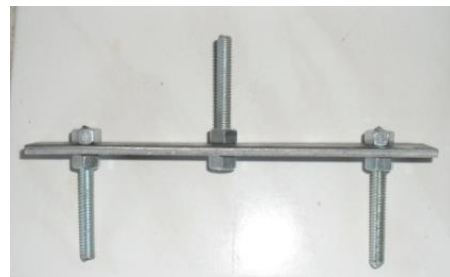


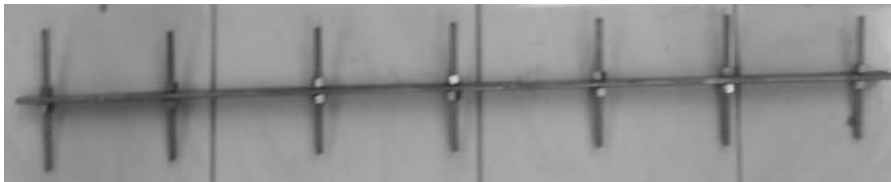
Fig. 4 Standard test setup



(a) W11, W12, and W41





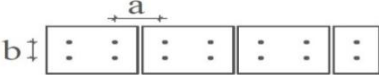
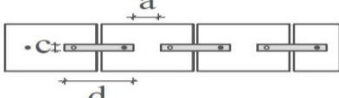
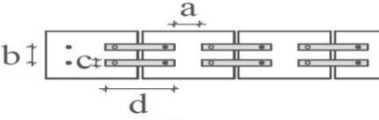
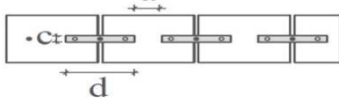
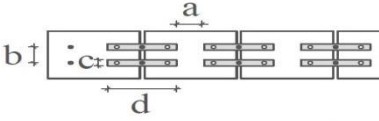
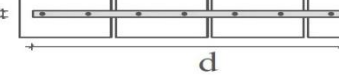

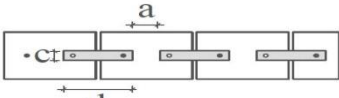
(b) W21 and W22



(c) W31 and W32

Fig. 5 The developed clamp models

Table 3 Description of the specimens

Masonry unit details	Test series	a (mm)	b (mm)	c (mm)	d (mm)
	W00	---	---	---	---
	W01	100	---	---	---
	W02	110	50	---	---
	W11	60	---	20	150
	W12	60	50	20	150
	W21	60	---	20	150
	W22	100	50	20	150
	W31	---	---	20	670
	W32	---	50	20	670
	W41	60	---	30	150

a: Horizontal distance between metal connectors b: Vertical distance between metal connectors c: Width of the clamps d: Length of the clamps

(W11-32) used 20 mm wide clamps. This approach was employed because sufficient improvement could not be provided by increasing clamp width. Each of the dowel holes was 20 mm deep with a diameter of 20 mm, while the clamps were 20 mm deep. Three different types of clamps were developed (Fig. 5), and these clamps were applied on the stone walls in single and double pieces. The general outline of the models is given in Table 3. The samples were identified as *W* (wall) followed by two numbers corresponding to the type and number of clamps, respectively.

The steps for constructing the stone masonry walls are given in Fig. 6. The holes in the stone units were drilled, and the clamps were subsequently inserted into the holes. The remaining parts





Fig. 6 Construction stages of stone masonry walls

were filled with cement grout. For the W01 and W02 specimens, 1-2 days were allowed between placing a dowel and bonding the wall. Natural tuff stones are relatively porous materials; therefore, before building, the stones were placed in a water tank for saturation. After 28-30 days curing, the specimens were placed in the test setup.

### 3. Experimental results and discussion

The stone masonry walls were subjected to a diagonal compression test, and both vertical and horizontal deformations were measured by displacement transducers. Test results are summarized in Table 4. In this table,  $P_{\max}$  is the maximum applied diagonal force,  $F_{\max}$  the is the maximum horizontal shear force,  $\tau_{\max}$  is the maximum shear stress,  $u_x$  and  $u_y$  are the horizontal and vertical displacement corresponding to  $\tau_{\max}$ ,  $\delta_y$  is determined as the drift value corresponding the shear strength of  $\tau_{\max}$ ,  $\delta_u$  is drift at 85% of the shear strength on the descending branch of the stress-drift relationship, and  $\mu$  is calculated as ratio of  $\delta_u$  to  $\delta_y$ . Chord shear modulus,  $G$ , was calculated from the shear stress-shear strain curve as the slope of the line between  $0.05 \tau_{\max}$  and  $0.33 \tau_{\max}$  (Building Code Requirements for Masonry Structures 2005).

The experimentally measured diagonal force,  $P$ , was transformed into shear stress,  $\tau$ , using Eq. (1), where  $t$  is the wall thickness,  $B$  is the wall length,  $H$  is the wall height, and  $\alpha$  is the angle between the lateral wall and the horizontal axis. Measured drift values,  $\delta$ , were calculated using



Table 4 Experimental test results

Test series	$P_{\max}$ (kN)	$F_{\max}$ (kN)	$\tau_{\max}$ (Mpa)	$u_x$ (mm)	$u_y$ (mm)	$\delta_u$ (%)	$\delta_y$ (%)	$\mu$	$G$ (Mpa)
W00	7.59	5.81	0.05	0.37	0.0001	0.0005	0.0004	1.25	407
W01	10.12	7.75	0.07	0.04	0.0001	0.0018	0.0010	2.80	273
W02	13.76	10.53	0.10	0.13	1.27	0.1736	0.1447	1.20	365
W11	16.88	12.93	0.13	4.07	1.41	0.5934	0.5679	1.04	105
W12	28.72	21.99	0.21	4.89	1.69	0.8510	0.7496	1.14	175
W21	32.46	24.85	0.24	4.15	6.91	1.0496	0.7311	1.44	30
W22	17.98	13.77	0.13	1.73	7.76	1.2990	0.9842	1.32	8
W31	42.41	32.47	0.32	7.84	7.35	0.5484	0.2277	2.41	4
W32	51.96	39.79	0.39	36.12	25.51	8.1925	6.3883	1.28	3
W41	19.48	14.92	0.15	3.63	13.75	2.0085	1.8018	1.12	4

Eq. (2), where  $\Delta v$  and  $\Delta h$  are the total displacements in the vertical and horizontal directions, and  $g$  is the gauge length (Ismail *et al.* 2011).

$$\tau = \frac{2P \cos \alpha}{(H + B)} \quad (1)$$

$$\delta = \frac{\Delta v + \Delta h}{2g} (\tan \alpha + \cot \alpha) \quad (2)$$

For the single clamp models W11, W21, and W31, the shear strength increased by 160%, 380%, and 540% on average compared to the W00 model and by 86%, 243%, and 357% on average compared to the W01 model. For the double clamp models W12, W22, and W32, the shear strength increased by 3200%, 160%, and 680% on average compared to the W00 model and by 110%, 30%, and 290% on average compared to the W01 model. The W41 model used a clamp that was 30 mm wide, and it increased the shear strength by only 15% compared to the W11 model. Therefore, the 20-mm clamp width was used for the rest of the models.

The unreinforced W00 as-built masonry wall behaved almost linearly up to the ultimate load when it suddenly failed at small deformations with a diagonal cracking failure mode. All wall specimens that were reinforced with clamps formed large displacements and reached high shear strength values. In the W01 and W02 models using dowels, the displacements increased, but the displacements could not be reached at higher shear forces.

The large increase in ductility for strengthened walls was ascribed to the reinforcement holding the stone masonry together and distributing stresses over larger areas. Using induced diagonal cracking, the ductility factor was determined. The ductility factor is highly sensitive to the calculated yield drift,  $\delta_y$ , which in the present tests showed significant variability, and for many of the tests, it was calculated as a notably small value. The large variations in observed  $\delta_y$  were ascribed to the redistribution of stresses and deformations throughout the highly heterogeneous material during the pre-peak loading phase. This redistribution resulted in a displacement that was measured along the compression diagonal, which is not representative of the true elastic drift. Certain modulus of rigidity values for the reinforced walls were lower than those of the unreinforced wall, but the walls with higher reinforcement ratios were stiffer.

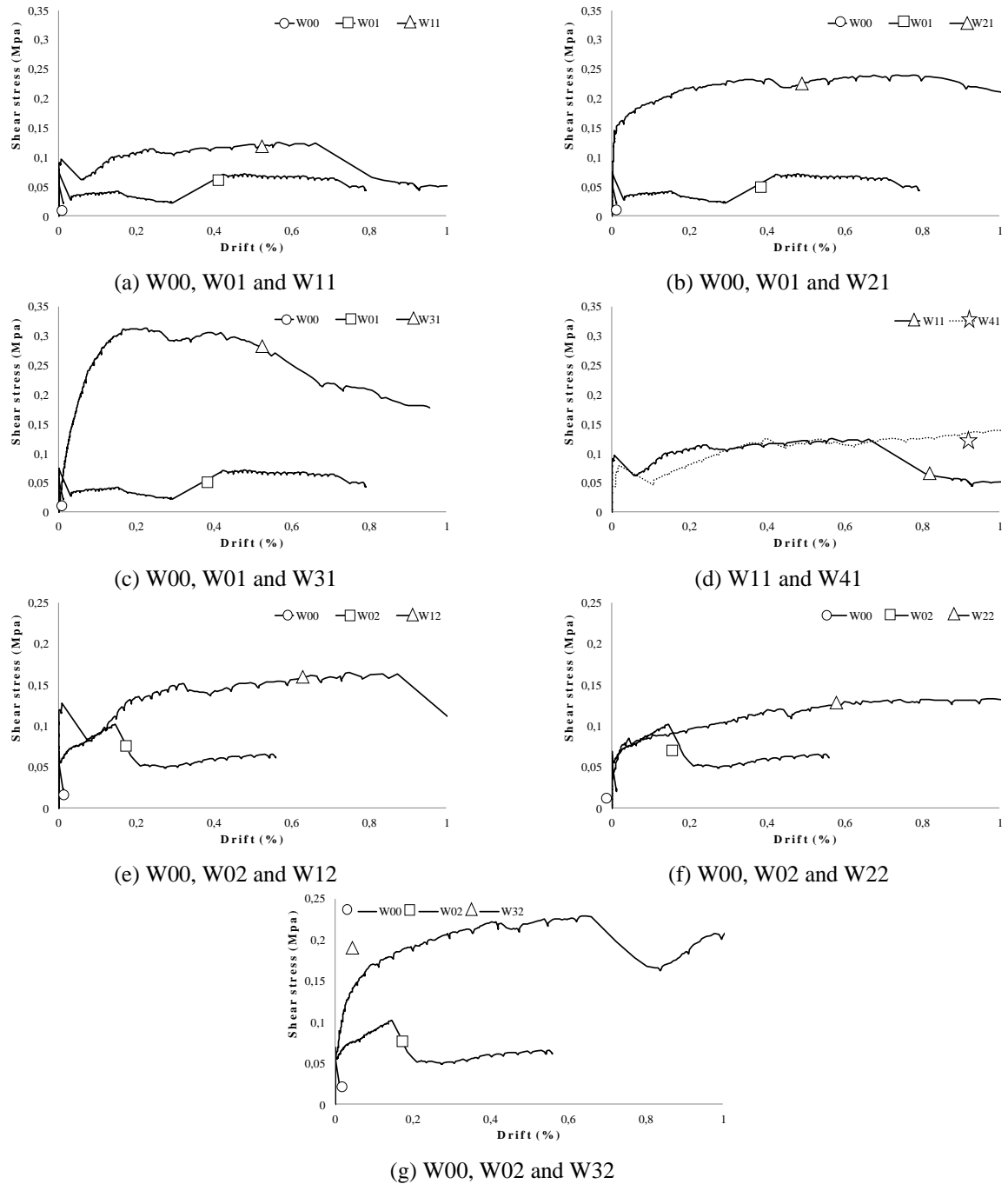


Fig. 7 Shear stress-drifts plots of masonry specimens

A maximum allowable drift limit of 0.5-0.6% is typically specified in design codes for masonry walls; therefore, the curves were plotted to a maximum drift of 1.0% (Fig. 7(a)-(g)) (TSB Committee E30 1998, Eurocode-6 2005). The shear stress–drift response of the as-built tested

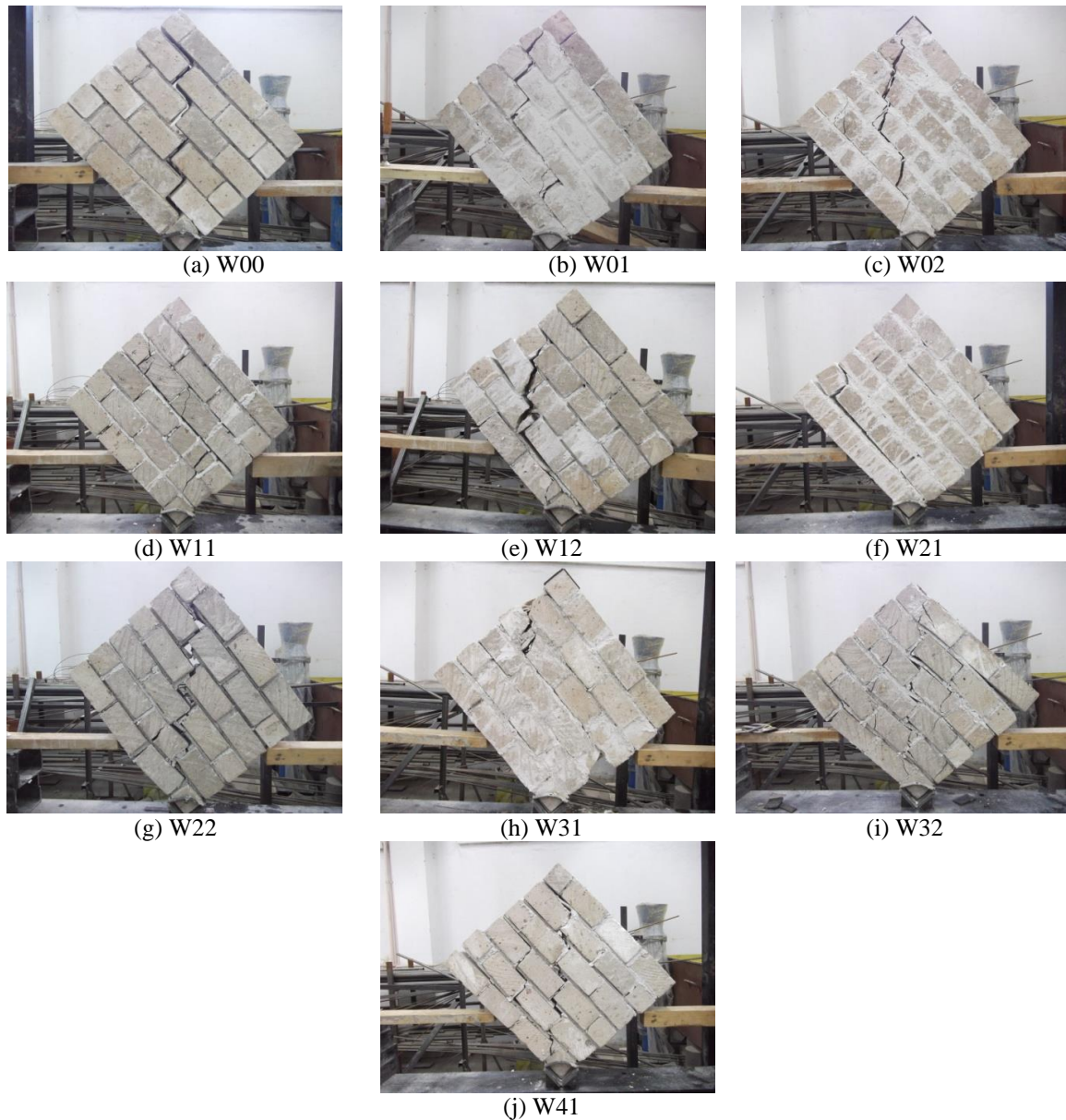


Fig. 8 The failure pattern of masonry specimens in diagonal compression

walls showed sudden strength degradation as cracking extended. In all strengthened walls, a linear-elastic behavior was observed up to the cracking point followed by a gradual decrease in the post-peak strength. Typical masonry walls are loaded axially due to their self-weight, and the bed joint sliding failure may not cause sudden complete loss of strength, as observed in this study. Moreover, masonry specimens having different configurations of metal connectors and reinforced walls are more ductile than unreinforced walls due to cracking in both the mortar joints and the masonry units, thereby generating slow failure of the wall (Fig. 8(a)-(j)).

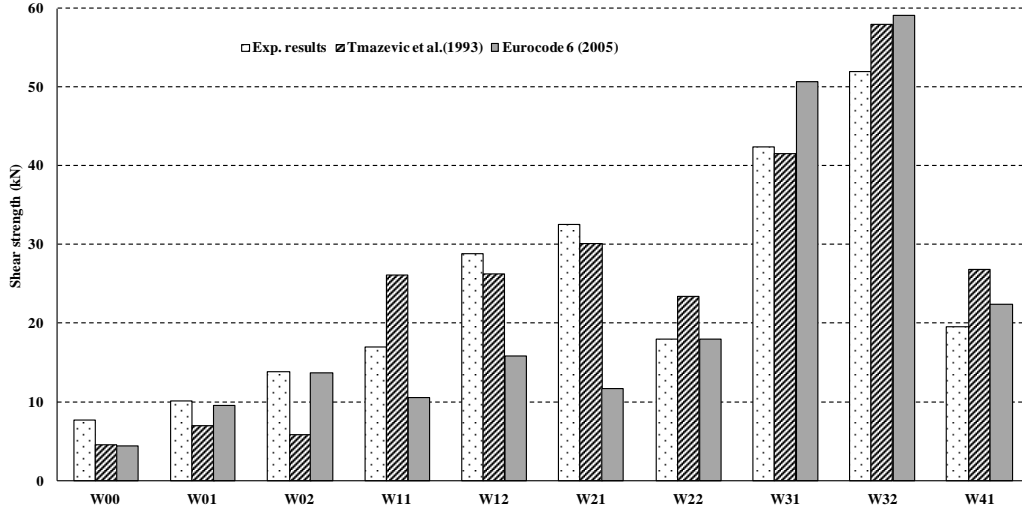


Fig. 9 Comparison between experimental and analytical predicted shear strength for masonry walls

#### 4. Comparison of shear strengths with the predictions and experimental results

Analytical models suggested for estimating the shear strengths of strengthened masonry walls are generally based upon the sum of the contributions of unreinforced masonry and reinforcement to the shear strength for mode II failure. Tomazevic *et al.* (1993) and Eurocode 6 (2005) suggest Eqs. (3) and (4) for predicting the shear strength of masonry reinforced with steel. These analytical equations are based on the linear effects of superposition, which are derived from the implicit assumption of plastic stress redistribution.

$$V_{Rd} = \left( \frac{0.9tdf'_{vko}}{1.5} + \sqrt{1 + \frac{\sigma}{f'_{vko}}} \right) + 0.4A_r f_{tk} \quad (3)$$

$$V_{Rd} = f_{vk} td + 0.9d\rho_t f_{tk} t \quad (4)$$

where

$$f_{vk} = f_{vko} + \mu\sigma \quad (5)$$

In these equations;  $V_{Rd}$  is the shear capacity of the masonry wall,  $t$  is the wall thickness,  $l$  is the wall length,  $d=0.8l$  is effective depth,  $\sigma$  is the vertical stress,  $f'_{vko}$  is the shear strength obtained from diagonal compressive tests,  $\rho_t$  is metal connectors ratio computed on the wall section,  $A_r$  is the area of the metal connectors,  $f_{tk}$  is the characteristic tensile stress of the metal connectors,  $f_{vk}$  is the shear strength obtained from the triplet shear tests,  $f_{vko}$  is the shear strength under zero compressive stress, and  $\mu$  is the friction coefficient. Initial shear strength at zero compressive stress  $f_{vko}$  can be determined by testing so called triplet specimens. Note that sliding test on triplets were not carried out on this study, therefore the default values of  $f_{vko}$  and  $\mu$  are given as 0.2 MPa and 0.4, respectively, by Eurocode 6 (2005), depending upon the characteristics of the masonry wall. The comparison between experimental and predicted values of the shear strength is reported in Fig. 9.

Table 5 Shear strength differences between the results of experimental study and other analytical methods

Test series	Experimental results	Eurocode 6 (2005)	Tomazevic <i>et al.</i> (1993)	Differences between experimental results and Eurocode 6 (2005)	Differences between experimental results and Tomazevic <i>et al.</i> (1993)
W00	7.59	4.40	4.50	43% decrease	41% decrease
W01	10.12	9.50	6.90	6% decrease	32% decrease
W02	13.76	13.70	5.70	1% decrease	58% decrease
W11	16.88	10.50	26.00	38% decrease	54% increase
W12	28.72	15.80	26.20	45% decrease	9% decrease
W21	32.46	11.60	30.00	64% decrease	8% decrease
W22	17.98	17.90	23.40	1% decrease	30% increase
W31	42.41	50.60	41.50	19% decrease	2% decrease
W32	51.96	59.10	57.90	14% increase	11% increase
W41	19.48	22.40	26.80	15% increase	37% increase

When comparing the analytical predictions and experimental results, it is clear that the empirical equations associated with the contribution of metal connectors should involve a parameter that takes into account the effective usable strain of metal connectors while considering potential failure modes.

Table 5 shows the results obtained from the experimental study and related analytical predictions. The results from the experimental study are given as a reference and the results from both analytical predictions are given as a percentage of the experimental results. According to Table 5, the comparison of the shear strengths between the experimental and Tomazevic *et al.* (1993) results are close to each other as much as 10% for the W12, W21, W31 and W32 specimens. Besides, the comparison of shear strengths between the experimental and Eurocode 6 (2005) results for W01, W02 and W22 specimens show less than %10 differences. The comparison of the shear strength results for the other specimens show approximately 50% difference. The experimental results of the single clamp specimens are well satisfied with the equation proposed by Tomazevic *et al.* (1993). Furthermore, the results of double clamp specimens are also well satisfied with the equation from Eurocode 6 (2005).

## 5. Conclusions

Various metal connectors were used that connect the walls vertically and horizontally for increase the shear strength of stone masonry walls. Three different new clamp designs were developed, and the shear strength was experimentally tested on stone masonry walls to determine if the clamps could increase the shear strength. These clamps were applied on stones in single and double units. At the end of experimental study examining the behavior of the stone masonry walls reinforced with clamp sheets, the following can be concluded:

- The type of test conducted (diagonal compression test) and the specimen dimensions seem to be an easy and efficient way to examine different strengthening configurations.
- The obtained experimental results generally agreed with the empirical formulas used.

All reinforced walls exhibited ductile failure modes and continued to resist load at the completion of testing. However, the unreinforced model, W00, presented a brittle failure along the

compressed diagonal with cracks that appeared suddenly in the mortar joints and in the stones, generating instantaneous wall failure.

- When the newly developed clamps (W11, W21, and W31) were applied on the stone masonry walls as a single unit, the unit substantially increased the shear strength and increased the energy absorption capacity of the walls by virtue of large displacements.

- When the newly developed clamps were applied on the stone masonry walls as a double unit, the unit reached greater shear strengths and displacements than when applied as a single unit.

- Although the newly developed clamp W41 was 30 mm wide, it could not provide any additional improvement than the 20-mm-wide W11 model. High shear forces and displacement values were attained in the W32 model. Therefore, this model is the most appropriate model for stone masonry walls.

- The shear strength results of the single clamp specimens are close to the calculated strength via the equation according to Tomazevic *et al.* (1993) and the results of the double clamp specimens are also close to the calculated strength from Eurocode 6 (2005).

- The three types of newly developed clamps can be used efficiently in stone masonry walls for newly built structures and for the restoration of historical structures.

## References

- Altin, S., Anil, O., Kara, M.E. and Kaya, M. (2008), "An experimental study on strengthening of masonry infilled RC frames using diagonal CFRP strips", *Compos., Part B*, **39**, 680-693.
- Arioglu, N. and Acun, S. (2006), "A research about a method for restoration of traditional lime mortars and plasters", *Build. Environ.*, **41**, 1223-1230.
- ASTM Committee E-519-02 (2002), *Standard test method for diagonal tension (shear) in masonry assemblages*, American Society for Testing and Materials International, USA.
- Augenti, N. and Parisi, F. (2010), "Constitutive models for tuff masonry under uniaxial compression", *J. Mater. Civil Eng.*, **22**(11), 1102-1111.
- Augenti, N. and Parisi, F. (2011), "Constitutive modeling of tuff masonry in direct shear", *Constr. Build. Mater.*, **25**, 1612-1620.
- British Standards Institution (2005), *Design of structures for earthquake resistance (BS EN 1998-3)*.
- Chiostrini, S. and Vignoli, A. (1992), "An experimental research program on the behavior of stone masonry structures", *J. Test Eval.*, **20** (3), 190-206.
- Corradi, M., Borri, A. and Vignoli, A. (2003), "Experimental study on the determination of strength of masonry walls", *J. Constr. Build. Mater.*, **17**(5), 325-337.
- El Gawady, M.A., Lestuzzi, P. and Badoux, M. (2006), "Aseismic retrofitting of reinforced masonry walls using FRP", *Compos., Part B, Eng.*, **37**(2-3), 148-162.
- Eurocode-6 EN 1996-1-1 (2005), *Design of masonry structures, part1-1: General rules for reinforced and unreinforced masonry structures*, Brussels.
- Gabor, A., Bennani, A., Jacquelin, E. and Lebon, F. (2006), "Modelling approaches of the in-plane shear behavior of unreinforced and FRP strengthened masonry panels", *Compos. Struct.*, **74**, 277-288.
- Isikdag, B. and Topcu, I.B. (2013), "The effect of ground granulated blast-furnace slag on the properties of Horasan mortar", *Constr. Build. Mater.*, **40**, 448-454.
- Ismail, N., Petersen, R.B., Masia, M.J. and Ingham, J.M. (2011), "Diagonal shear behavior of unreinforced masonry wallets strengthened using twisted steel bars", *Constr. Build. Mater.*, **25**, 4386-4393.
- Ismail, N., Petersen, R.B., Masia, M.J. and Ingham, J.M. (2012), "Finite element modeling of unreinforced masonry shear wallets strengthened using twisted steel bars", *Constr. Build. Mater.*, **33**, 14-24.
- Kalali, A. and Kabir, M.Z. (2012), "Experimental response of double-wythe masonry panels strengthened with glass fiber reinforced polymers subjected to diagonal compression tests", *Eng. Struct.*, **39**, 24-37.

- Kourkoulis, S.K. and Pasiou, E.D. (2009), "Epistyles connected with I connectors under pure shear", *J. Serbian Soc. Comput. Mech.*, **3**(2), 81-99.
- Papadopoulos, K.A. (2006), "The restoration study of the connections between the stone blocks in the steps of the temple of Apollo Epikourios", *Struct. Anal. Histori. Constr.*, New Delhi, India, November.
- RILEM (1994), *LUMB6-Diagonal tensile strength tests of small wall specimens*, Tech Rep, RILEM.
- Shariati, M., Sulong, N.H.R., Suhatri, M., Shariati, A., Khanouki, M.M.A. and Sinaei, H. (2012), "Behaviour of C-shaped angle shear connectors under monotonic and fully reversed cyclic loading: an experimental study", *Mater. Des.*, **41**, 67-73.
- The Masonry Standards Joint Committee (2005), Building Code Requirements for Masonry Structures (ACI 530-05 & 530.1-05 / ASCE 5-05 & 6-05 / TMS 402-05 & 602-05).
- Tomazevic, M., Lutman, M. and Petrovic, L. (1993), *In plane behavior of reinforced masonry walls subjected to cyclic lateral loads*, Report to the ministry of science and technology of Republic of Slovenia, parts 1 and 2. Ljubljana, Slovenia.
- Tomazevic, M. (1999), *Earthquake-resistant design of masonry buildings*, Imperial College Press, London, England.
- Toumbakari, E.E. (2008), "The Athens Parthenon: Analysis and interpretation of the structural failures in the orthostate of the northern wall", *Struct. Anal. Histori. Constr.*, United Kingdom.
- Turkish Standard. TS EN 196-1 (2002), *Methods of testing cement - Part 1: Determination of strength*, Ankara, Turkey.
- Turkish Standard. TS 699 (2009), *Natural building stones - Methods of inspection and laboratory testing*, Ankara, Turkey.
- TSB Committee E30 (1998), *Earthquake resistant design: national construction code, Technical Standard for Buildings*, Lima.